Citrulline enteral administration markedly reduces immunosuppressive extrafollicular plasma cell differentiation in a preclinical model of sepsis

Juliette Gauthier, Murielle Grégoire, Florian Reizine, Mathieu Lesouhaitier, Yoni Desvois, Gevorg Ghukasyan, Caroline Moreau, Patricia Ame, Karin Tarte, J.-M. Tadié, et al.

▶ **To cite this version:**

Juliette Gauthier, Murielle Grégoire, Florian Reizine, Mathieu Lesouhaitier, Yoni Desvois, et al.. Citrulline enteral administration markedly reduces immunosuppressive extrafollicular plasma cell differentiation in a preclinical model of sepsis. European Journal of Immunology, 2023, 53 (3), pp.2250154. 10.1002/eji.202250154 . hal-03923239

HAL Id: hal-03923239
https://hal.science/hal-03923239

Submitted on 4 Jul 2023

HAL is a multi-disciplinary open access archive for the deposit and dissemination of scientific research documents, whether they are published or not. The documents may come from teaching and research institutions in France or abroad, or from public or private research centers.

L'archive ouverte pluridisciplinaire **HAL**, est destinée au dépôt et à la diffusion de documents scientifiques de niveau recherche, publiés ou non, émanant des établissements d'enseignement et de recherche français ou étrangers, des laboratoires publics ou privés.

Distributed under a Creative Commons Attribution - NonCommercial - NoDerivatives 4.0 International License

Check for updates

European Journal of Immunology Clinical·Basic·Translational

Immunomodulation and immune therapies

Basic

Research Article

Citrulline enteral administration markedly reduces immunosuppressive extrafollicular plasma cell differentiation in a preclinical model of sepsis

Juliette Gauthier[1], *Murielle Grégoire*[1,2], *Florian Reizine*[1,2,3], *Mathieu Lesouhaitier*[1,2,3], *Yoni Desvois*[1], *Gevorg Ghukasyan*[4], *Caroline Moreau*[5,6], *Patricia Amé*[1,2], *Karin Tarte*[1,2], *Jean-Marc Tadié*[#1,2,3] *and Céline Delaloy*[#1]

[1] UMR INSERM S1236, LabEx IGO, Univ Rennes, EFS, Rennes, France
[2] CHU Rennes, SITI Laboratory, Pôle Biologie, Rennes, France
[3] CHU Rennes, Maladies Infectieuses et Réanimation Médicale, Rennes, France
[4] Univ Rennes, UMS Biosit, H2P2 Platform, Rennes, France
[5] CHU Rennes, Laboratoire de Biochimie, Pôle Biologie, Rennes, France
[6] Univ Rennes, INSERM, EHESP, IRSET, UMR S1085, Rennes, France

The sustained immunosuppression associated with severe sepsis favors an increased susceptibility to secondary infections and remains incompletely understood. Plasmablast and plasma cell subsets, whose primary function is to secrete antibodies, have emerged as important suppressive populations that expand during sepsis. In particular, sepsis supports CD39^{hi} plasmablast metabolic reprogramming associated with adenosine-mediated suppressive activity. Arginine deficiency has been linked to an increased risk of secondary infections in sepsis. Overcoming arginine shortage by citrulline administration efficiently improves sepsis-induced immunosuppression and secondary infections in the cecal ligation and puncture murine model. Here, we aimed to determine the impact of citrulline administration on B cell suppressive responses in sepsis. We demonstrate that restoring arginine bioavailability through citrulline administration markedly reduces the dominant extrafollicular B cell response, decreasing the immunosuppressive LAG3^{+} and CD39^{+} plasma cell populations, and restoring splenic follicles. At the molecular level, the IRF4/MYC-mediated B cell reprogramming required for extrafollicular plasma cell differentiation is shunted in the splenic B cells of mice fed with citrulline. Our study reveals a prominent impact of nutrition on B cell responses and plasma cell differentiation and further supports the development of citrulline-based clinical studies to prevent sepsis-associated immune dysfunction.

Keywords: animal model · citrulline · immunosuppression · regulatory plasma cell · sepsis

Additional supporting information may be found online in the Supporting Information section at the end of the article.

Correspondence: Jean-Marc Tadié and Dr. Céline Delaloy
e-mail: jeanmarc.tadie@chu-rennes.fr; celine.delaloy@univ-rennes1.fr

[#]Lead authors

© 2022 The Authors. *European Journal of Immunology* published by Wiley-VCH GmbH

This is an open access article under the terms of the Creative Commons Attribution-NonCommercial-NoDerivs License, which permits use and distribution in any medium, provided the original work is properly cited, the use is non-commercial and no modifications or adaptations are made.

Introduction

In addition to multi-organ dysfunction, sepsis induces prolonged depression of immune responses that accounts for increased susceptibility to infections and late mortality [1]. The paralysis of the immune system affects both innate and adaptive immune responses and results from the reprogramming of multiple immune cell subsets. Among them, B cells experience a number decrease in the cecal ligation and puncture (CLP) murine septic model [2, 3] as well as in septic shock patients [4] and B cell apoptosis has been proposed as a mechanism responsible for B cell depletion in sepsis [5–7]. Beyond lymphopenia, B cell functions are shaped during sepsis, supporting acquired immunosuppression.

First, antibody production is impaired in sepsis. In response to infections, activated B cells proliferate and differentiate rapidly into short-lived plasmablasts (PB) and plasma cells (PC), producing low-affinity antibodies through the extrafollicular (EF) pathway. Activated B cells can also interact with $CD4^+$ T cells which provide necessary help for their commitment toward the germinal center (GC) reaction. In the latter case, B cells relocate to the follicle center to undergo expansion and affinity maturation to produce high-affinity long-lived PC and memory B cells. The magnitude and duration of the EF and GC responses rely on signals from the microenvironment [8], epigenetic and transcriptional cues [9] as well as on metabolic reprogramming [10]. In the CLP model, impaired GC formation results in a reduced antigen-specific antibody response [2, 3, 11]. This arises as a result of specific defects in $CD4^+$ T cell subset providing help to B cell [3]. In line with this, adoptive transfer studies have demonstrated the absence of B-cell intrinsic defects in CLP mice at the origin of defective T-cell-dependent B cell responses [11].

In addition to their role in antibody production and antigen presentation, B cells can exhibit either pro-inflammatory or suppressive functions, hence contributing to the maintenance and regulation of immune homeostasis [12]. Several evidence support the idea that septic immunosuppression may be driven by regulatory subsets of B cells. Defined by the expression of the hallmark immunoregulatory cytokine IL-10, regulatory B cells are increased in the peripheral blood of septic shock patients [4]. Several studies have also linked IL-10 production by B cells to their differentiation into PC [13, 14]. PC, whose primary function is to secrete antibodies, are very heterogeneous subsets of differentiated B cells. They are characterized by their maturation stage—proliferative PB giving rise to the more mature PC, their Ig isotype expression, and their functions [15]. Immunosuppressive populations of PB/PC expressing IL-10 and expanding during infections have been described [13]. Importantly, sepsis was shown to support $CD39^{hi}$ PB expansion responsible for adenosine-mediated suppressive activity [16]. In line with this, septic patients presented with marked plasmacytosis early after the onset of septic shock [4, 17]. Furthermore, a subpopulation of natural regulatory PC expressing LAG3 have been shown to suppress immunity through IL-10 production [18]. However, regulatory PB/PC ontogenesis after sepsis remains to be studied.

Therapeutic strategies are needed to restore immune system homeostasis after sepsis. Recent evidence supports the concept that nutritional intervention can enhance protective immunity while also limiting aberrant inflammatory responses [19]. Arginine deficiency resulting from enhanced arginase activity in sepsis has been linked to an increased risk of recurrent infections [20, 21]. In a cellular damage context, arginase released from the mitochondria of dead cells was shown to switch NK and T cell responses toward a regulatory function [22]. Importantly, overcoming the arginine shortage by citrulline enteral administration was shown to efficiently improve sepsis-induced immunosuppression and secondary infections in the CLP model [23]. Expansion of regulatory T cell (Treg) and myeloid-derived suppressor cell (MDSC) immunosuppressive populations in sepsis is reduced with a citrulline diet. In addition, T cell mitochondrial dysfunction is restored with diet rescues T cell effector functions.

In this study, we aimed to define regulatory PB/PC ontogenesis within 5 days after CLP and the impact of citrulline treatment on B cell-mediated immunosuppressive functions in sepsis. We show that restoring arginine bioavailability markedly reduces the dominant EF PC differentiation, thus depleting the immunosuppressive $LAG3^+$ and $CD39^{hi}$ PC subsets, both expanded in CLP, and restoring splenic follicles, mechanisms that could contribute significantly to the beneficial effect of citrulline.

Results

Expansion of EF PB and PC following CLP

To study immunosuppressive B-cell responses in the context of sepsis-induced arginine depletion, we used the CLP model [23]. The experimental approach is shown in Fig. 1A B cell responses were studied on day 5 post-surgery. Despite B cell lymphopenia in the spleen of CLP compared to sham mice (average 47% vs 38% of B cells in sham and CLP, respectively, $p = 0.0032$; Fig. 1B), CLP mice displayed elevated frequency of $CD138^+$ $TACI^+$ differentiated B cells (average 0.42% vs 3.6% PB/PC among live cells in sham and CLP respectively, $p<0.0001$; Fig. 1C). When looking at the maturation states of these differentiated B cells by flow cytometry analysis according to Pracht *et al.* protocol [24] (Supp Fig. 1B), they corresponded mainly to PB ($B220^+$ $CD19^+$, average 1.74% among live cells in CLP vs. 0.19% in sham, $p < 0.0001$) and to a lesser extent to early PC ($B220^{lo}$ $CD19^+$, average 1.08% among live cells in CLP vs. 0.08% in sham, $p<0.0001$) and mature resting PC ($B220^{lo}CD19^-$, average 0.22% among live cells in CLP vs 0.03% in sham, $p<0.0001$; Fig. 1D). Because marked plasmacytosis is described in septic patients [4], we analyzed PB/PC in the peripheral blood of CLP mice and did not observe CLP-induced plasmacytosis at this early time point after surgery (Fig. 1E). Instead, immunofluorescent staining of $CD138^+$ PB/PC in spleen sections revealed their accumulation in the red pulp within the EF foci (Fig. 1F). Consistent with an early EF B cell response, the IgM level was increased up to 20-fold in the CLP plasma compared to sham ($p<0.0001$; Fig. 1G). An increase in IgG1 and IgA

© 2022 The Authors. *European Journal of Immunology* published by Wiley-VCH GmbH

15214141, 2023, 3, Downloaded from https://onlinelibrary.wiley.com/doi/10.1002/eji.202250154 by Université De Rennes 1 BU Campus Beaulieu - Bât. 40, Wiley Online Library on [04/07/2023]. See the Terms and Conditions (https://onlinelibrary.wiley.com/terms-and-conditions) on Wiley Online Library for rules of use; OA articles are governed by the applicable Creative Commons License

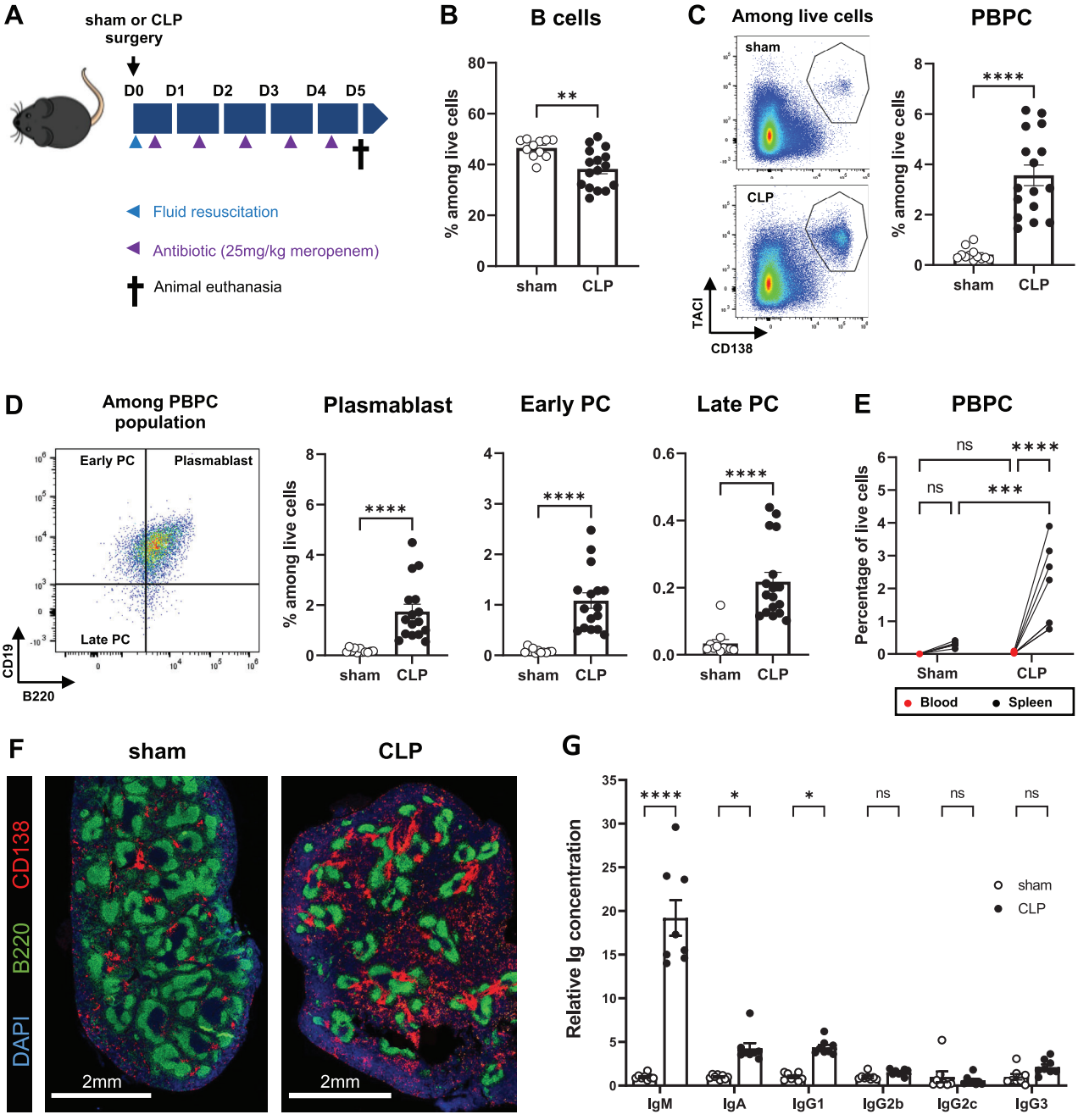

Figure 1. CLP induces reduction of B cell frequency and EF PC differentiation. (A) Experimental design. Mice underwent CLP surgery or sham laparotomy and received fluid resuscitation (blue arrow) at day 0 (D0) and 25mg/kg of meropenem antibiotic (purple arrow) every day until euthanasia (black cross) 5 days post-surgery. Blood and spleen were harvested from mice on day 5. **(B)** splenic B cells ($CD19^+$ $B220^+$ $TACI^-$ $CD138^-$) frequency. Combined data from 2 independent experiments, each performed with 6–8 mice per group, are shown. **(C)** Frequency of splenic $TACI^+$ $CD138^+$ PB/PC in sham and CLP mice. The gate selects the PB/PC population from among live cells. Combined data from 2 independent experiments, each performed with 6–8 mice per group, are shown. **(D)** Dot plots represent splenic $TACI^+$ $CD138^+$ PB/PC depending on their expression of CD19 and B220. The gates placed according to positive and negative cells (Supp Fig. 1B) select $B220^+$ $CD19^+$ PB, $B220^{lo}$ $CD19^+$ early PC, and $B220^{lo}$ $CD19^{lo}$ late PC. Histograms represent the percentage of PB (left), early PC (middle), and late PC (right) among live cells in sham and CLP mice. Combined data from 2 independent experiments, each performed with 6–8 mice per group, are shown. **(E)** Histogram represents the percentage of $TACI^+$ $CD138^+$ PB/PC among live cells from spleen (black) and blood (red) of sham and CLP mice (6-8 mice per group, two-way ANOVA with Tukey correction). **(F)** Immunofluorescences of a representative splenic tissue section from sham and CLP mice (6 to 8 mice per group) stained with DAPI (blue) and antibodies targeting B220 (green) and CD138 (red). Scale bars, 2 mm. **(G)** Histogram represents the relative immunoglobulin concentrations in plasma of sham and CLP mice (8 mice per group, from 2 independent experiments; two-way ANOVA with Tukey correction). Values were determined using a ratio of immunoglobulin concentration (IgM, IgA, IgG1, IgG2b, IgG2c, IgG3) measured in the plasma of the indicated mice relative to the average immunoglobulin concentration measured in sham mice. Symbols represent one individual mouse, and bars indicate mean ± SEM. ns = non-significant, ** $p<0.01$, *** $p<0.001$, **** $p<0.0001$ (Mann-Whitney test unless specified).

© 2022 The Authors. *European Journal of Immunology* published by Wiley-VCH GmbH

15214141, 2023, 3, Downloaded from https://onlinelibrary.wiley.com/doi/10.1002/eji.202250154 by Université De Rennes 1 BU Campus Beaulieu - Bât. 40, Wiley Online Library on [04/07/2023]. See the Terms and Conditions (https://onlinelibrary.wiley.com/terms-and-conditions) on Wiley Online Library for rules of use; OA articles are governed by the applicable Creative Commons License

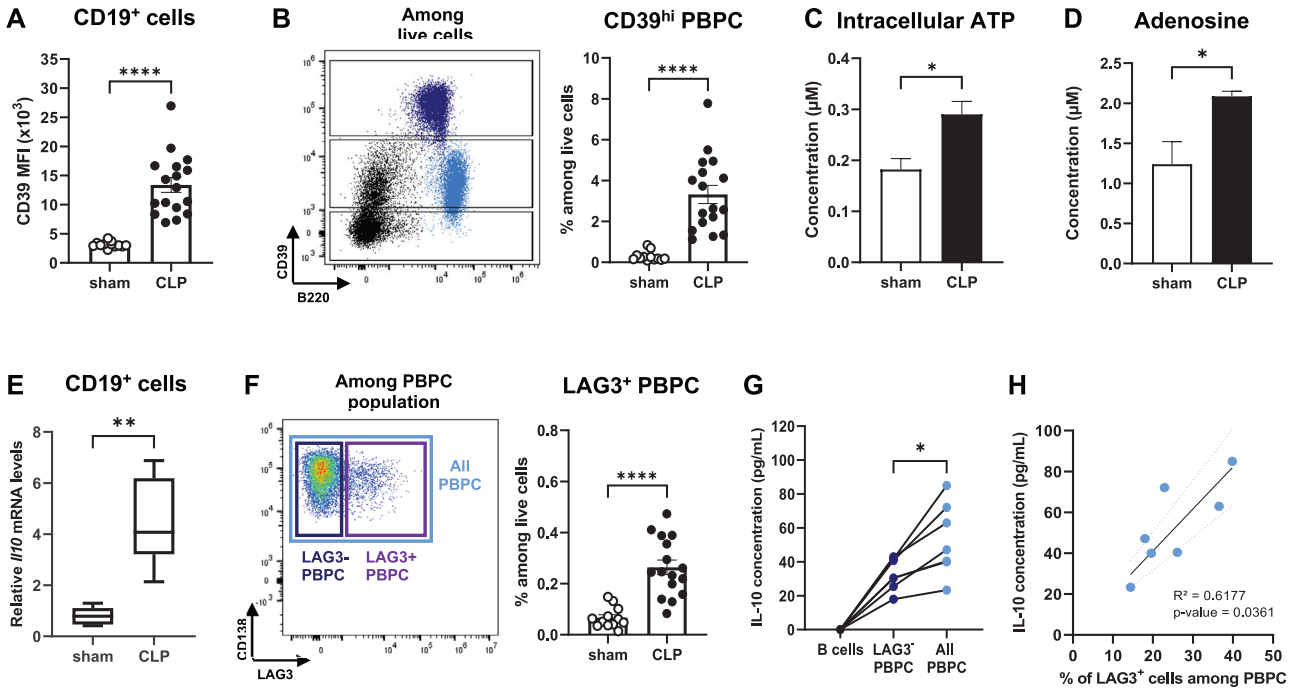

Figure 2. Immunosuppressive CD39^{hi} and LAG3^{+} PB/PC expansion in CLP mice. (A) Flow cytometry analysis of CD39 expression on splenic CD19^{+} B cells and TACI^{+} CD138^{+} PB/PC. Histogram shows the CD39 mean fluorescence intensity (MFI) of CD19^{+} splenic B cells analyzed in sham and CLP mice. **(B)** Dot plot shows the overlay of PB/PC (dark blue), B cells (light blue), and splenic non PB/PC, non-B cells (black) according to their expression of CD39 and B220. The gates from the bottom to the top (as determined in supp Fig. 1C) select the CD39^{-}, CD39^{+} and CD39^{hi} cells. Histogram represents the percentage of splenic CD39^{hi} PB/PC among live cells. **(A-B)** Combined data from 2 independent experiments, each performed with 6–8 mice per group, are shown. **(C)** Bar graph represents the intracellular ATP concentration (µM) measured by luminometric assay in splenic CD19^{+} cells from 6 sham and 8 CLP (N = 1). **(D)** Bar graph shows the adenosine concentration (µM) measured by fluorometric assay in the plasma of indicated mice (10 sham and 7 CLP, N = 2). **(E)** Relative *Il10* mRNA expression measured in splenic CD19^{+} cells from the indicated group of animals (5 sham and 7 CLP). Relative expression was normalized to *B2m*. Bars represent median ± min to max. **(F)** Flow cytometry analysis of LAG3^{+} PB/PC (TACI^{+} CD138^{+}). The dot plot represents PB/PC depending on their expression of CD138 and LAG3. The purple gate selects the LAG3^{+} PB/PC, the dark blue gate selects LAG3^{-} PB/PC and the light blue gate selects all PB/PC. The two blue gates (dark and light) are used to sort these populations from 7 CLP mice analyzed in **(G-H)**. Histogram showing the percentage of LAG3^{+} PB/PC among live cells for each group. Combined data from 2 independent experiments, each performed with 6–8 mice per group, are shown. **(G)** IL-10 concentration (pg/mL) measured by ELISA in the supernatant of sorted LAG3^{-} PB/PC or all PB/PC from 7 CLP mice after 24 h of culture with LPS and anti-BCR (Wilcoxon test). **(H)** Correlation between the percentage of LAG3^{+} cells among PB/PC in the spleen of 7 CLP mice and the amount of IL-10 (concentration in pg/mL) secreted by all PB/PC in the culture media during 24 h (Pearson test). **(A–F)** Bars represent means ± SEM (Mann-Whitney test). Symbols represent one individual mouse. * $p<0.05$, ** $p<0.01$, *** $p<0.001$, **** $p<0.0001$.

was also observed in mice following CLP (average 4.2- and 4.3-fold increase of IgA and IgG1, respectively, in CLP compared to sham, $p = 0.0349$ and $p = 0.0249$, respectively), and no significant difference was observed in IgG2b, IgG2c, and IgG3 isotype levels between sham and CLP (Fig. S2).

CLP induces immunosuppressive CD39^{hi} PB/PC expansion

We next measured CD39 expression using flow cytometry. CD39 expression was significantly higher in splenic CD19^{+} B cell cells from CLP than in sham mice (average CD39 MFI: 3.13×10^3 vs 13.37×10^3 in sham and CLP respectively, $p<0.0001$; Fig. 2A). As expected, CD39 was highly expressed by the differentiated PB/PC subset and the frequency of this CD39^{hi} PB/PC subset was increased in CLP (average 0.29% vs 3.32% CD39^{hi} PB/PC in sham and CLP respectively, $p<0.0001$; Fig. 2B). Consistent with the metabolic shift required for PC differentiation, CD19^{+} splenic cells from CLP mice contained higher amounts of ATP (average 0.18 µM in sham vs. 0.29 µM in CLP, $p = 0.0177$; Fig. 2C). Because CD39 drives immunosuppression through ATP hydrolysis responsible for the increased circulating adenosine [16], we measured adenosine in plasma and observed adenosine accumulation in septic mice (average 1.24 µM in sham vs 2.01 µM in CLP, $p = 0.0320$; Fig. 2D). Taken together, immunosuppression mediated by CD39-expressing PB/PC takes place as soon as day 5 post-CLP.

Immunosuppressive LAG3^{+} PB/PC are expanded in CLP

Gene expression profiling of CD19^{+} splenic B cells revealed a 5.7-fold increase of *Il10* expression in CLP compared to sham, suggesting that B or PB/PC subsets could have immunoregulatory functions through IL-10 production in sepsis ($p<0.0001$; Fig. 2E). We thus measured by flow cytometry the expansion of LAG3^{+} regulatory PB/PC in the spleen of CLP mice compared to sham mice.

© 2022 The Authors. *European Journal of Immunology* published by Wiley-VCH GmbH

15214141, 2023, 3, Downloaded from https://onlinelibrary.wiley.com/doi/10.1002/eji.202250154 by Université De Rennes 1 BU Campus Beaulieu - Bât. 40, Wiley Online Library on [04/07/2023]. See the Terms and Conditions (https://onlinelibrary.wiley.com/terms-and-conditions) on Wiley Online Library for rules of use; OA articles are governed by the applicable Creative Commons License

15214141, 2023, 3, Downloaded from https://onlinelibrary.wiley.com/doi/10.1002/eji.202250154 by Université De Rennes 1 BU Campus Beaulieu - Bât. 40, Wiley Online Library on [04/07/2023]. See the Terms and Conditions (https://onlinelibrary.wiley.com/terms-and-conditions) on Wiley Online Library for rules of use; OA articles are governed by the applicable Creative Commons License

An average 4-fold increase of LAG3$^+$ PB/PC was observed in CLP ($p<0.0001$; Fig. 2F). To confirm their regulatory function in our CLP model, we sorted total CD138$^+$ TACI$^+$ PB/PC and CD138$^+$ TACI$^+$ LAG3$^-$ PB/PC from spleen and evaluated their ability to produce IL-10. In agreement with the immunosuppressive function of LAG3$^+$ PC, IL-10 was mainly produced by the population containing LAG3$^+$ PB/PC ($p<0.0156$; Fig. 2G), and a positive correlation was observed between LAG3$^+$ PB/PC frequency and IL-10 concentration measured in the media 24 h after *in vitro* stimulation ($p = 0.0361$; Fig. 2H). Thus LAG3$^+$ PB/PC expansion contributes to immunosuppression in CLP.

Citrulline administration decreases EF humoral response in sepsis

To study the impact of citrulline treatment on these B cell subsets, we treated CLP animals with either a placebo, 150mg/kg of citrulline, or 150mg/kg of arginine every day for five days [23] (Fig. 3A). In agreement with our previous results, citrulline enteral administration restored the arginine deficiency measured in the plasma of CLP mice following diet ($p = 0.0331$; Fig. 3B). Survival rates were similar in mice undergoing CLP and placebo compared to CLP complemented with citrulline or arginine, with a mortality of 14% (8/58) within the first five days following CLP surgery + placebo versus 14% (8/58) in CLP + citrulline and 26% (13/50) in CLP + arginine (Fig. S3). There was no difference between the three groups of mice receiving either citrulline, arginine, or placebo after CLP in terms of B cell frequency in the spleen, measured by flow cytometry (CD19$^+$ B220$^+$ excluding TACI$^+$ CD138$^+$ PB/PC, Fig. 3C). In contrast, citrulline administration strikingly decreased PB/PC frequency in the spleen (average 3.93% vs 0.97% of PB/PC in CLP + placebo and CLP + citrulline, respectively, $p = 0.0027$; Fig. 3D). The IgM, IgA, and IgG1 plasma levels were equally decreased by the citrulline treatment (Fig. 3E). Conversely, arginine administration did not impact the humoral response (Fig. 3D-E). Thus, the EF response triggered by CLP was reduced when arginine bioavailability was restored with a citrulline diet. Consistent with the overall effect of citrulline on the PB/PC population, the frequency of CD39^{hi} subset was decreased with citrulline (average 3.47% in CLP + placebo vs 0.83% in CLP + citrulline, $p = 0.0006$; Fig. 3F). In addition, CD39 expression on PB/PC decreased significantly with citrulline treatment (average 165×10^3 MFI in CLP + placebo vs 123×10^3 MFI in CLP + citrulline, $p = 0.0006$; Fig. 3G). We next wanted to determine whether citrulline contributes to reverse adenosine accumulation in septic mice. While citrulline treatment did not modify the amount of ATP in CD19$^+$ cells, excluding a major cell intrinsic metabolic reprogramming (Fig. 3H), it tended to decrease plasma adenosine accumulation in septic mice (average adenosine: 1.77 μM in CLP + placebo vs. 1.26 μM in CLP + citrulline, $p = 0.0650$; Fig. 3I). Lastly, citrulline administration significantly reduced the expansion of LAG3$^+$ regulatory PB/PC in the spleen of CLP mice (0.31% vs 0.17% of LAG3$^+$ PB/PC in CLP + placebo and CLP + citrulline, respectively, $p = 0.0152$; Fig. 3J). In line with this result, citrulline contributed to a trend toward a reduction in *Il10* expression in CD19$^+$ splenic cells ($p = 0.0823$; Fig. 3K). Together, these data reveal that citrulline treatment can counteract the early drivers of PC-mediated immunosuppression in sepsis.

Citrulline administration counteracts EF PC fate programming in CLP

Next, we sought to determine the cause of the reduced PB/PC frequency induced by citrulline treatment. Following CLP, both MHC-II and CD86, markers of B cell activation, were increased in CD19$^+$ splenic B cells, but citrulline-enriched diet did not modify their expression (Fig. 4A). Accordingly, *Mki67* expressed by proliferative cells was markedly upregulated in CD19$^+$ splenic B cells from CLP mice (average 5.4-fold increase of *Mki67* in CLP compared to sham, $p = 0.0025$; Fig. 4B), but citrulline enriched diet did not significantly impact *Mki67* expression or the frequency of proliferative Ki-67$^+$ cells within the B cell and the PB/PC subsets (Fig. 4C). We then tested whether PB/PC reduction was the result of increased PB/PC death and found that citrulline treatment did not affect the apoptosis of B cells nor PB/PC compared with the placebo control group (Fig. 4D). Since B cell fate programming toward the EF path happens early during the initial stages of B cell activation and is under the control of transcriptional regulation [25], we aimed to determine whether citrulline treatment contributes to B cell fate reprogramming. We performed gene expression profiling of CD19$^+$ splenic cells for critical factors involved in this process and identified *Irf4* repression with a citrulline enriched diet ($p = 0.0087$; Fig. 4E). Sustained and high *Irf4* expression was shown to promote PC differentiation while antagonizing the GC path [26], a mechanism that requires IRF4-induced MYC target genes [27]. In agreement with *Irf4* downregulation, *Myc* expression was significantly decreased in CD19$^+$ cells ($p = 0.0087$), and its target genes *Cdc25a* and *Ccnd2* were downregulated with citrulline diet ($p = 0.0284$ for *Cdc25a* and $p = 0.0519$ for *Ccnd2* expression; Fig. 4E). These data suggest that the IRF4/MYC pathway, controlling the rapid differentiation of activated B cells into PC, is shunted following citrulline diet.

Reappearance of B and T follicles following citrulline diet

Since IRF4 is a crucial transcription factor involved in the bifurcation fate of B cells towards PC differentiation or the GC reaction [28, 25], we hypothesized that citrulline diet may favour the GC response. Histological analysis revealed structural changes in the spleen 5 days post-CLP (Fig. 5A). Follicles were scattered farther apart from each other, with significantly smaller B follicle areas ($p = 0.0027$) and T cell zones ($p = 0.0082$) in CLP-exposed mice compared with sham (Fig. 5B). These modifications were reversed with citrulline treatment ($p = 0.0830$ for B cell follicle and $p = 0.0281$ for T cell areas; Fig. 5B). In agreement with reappearance of B and T follicles, *Ccr7* expression, a chemokine

© 2022 The Authors. *European Journal of Immunology* published by Wiley-VCH GmbH

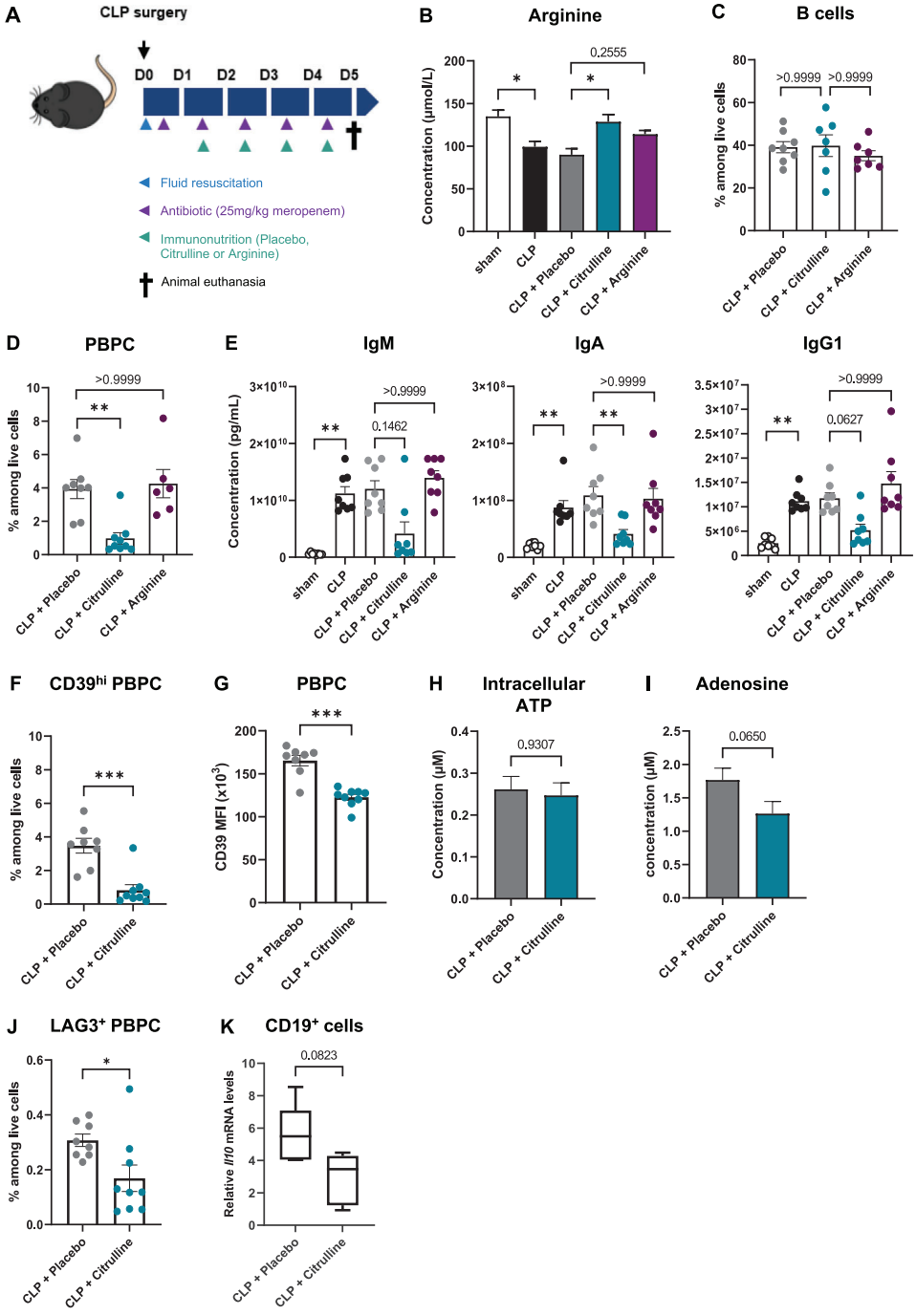

Figure 3. Regulatory PB/PC expansion induced by CLP is markedly inhibited by citrulline administration. (A) Experimental design of immunonutrition. Mice that underwent CLP surgery received fluid resuscitation (blue arrow) and antibiotic (purple arrows) and were enterally fed with either an isonitrogenous placebo, 150mg/kg of citrulline or 150mg/kg of arginine every day (green arrows). Blood and spleen were harvested from mice 5 days postsurgery. **(B)** Bars represent the concentration of arginine (µmol/L) measured in the plasma of indicated mice. **(C)** Flow cytometry analysis of the percentage of splenic B cells ($CD19^+$ $B220^+$ $TACI^-$ $CD138^-$). **(D)** Frequency of splenic PB/PC ($TACI^+$ $CD138^+$) among live cells. **(E)** Histograms represent IgM, IgA, and IgG1 concentrations (pg/mL) in the plasma of the indicated group of mice. **(F)** Histogram representing the percentage of splenic $CD39^{hi}$ PB/PC among live cells. **(G)** Histogram showing the CD39 MFI of PB/PC for each indicated group of animals. **(H)** Intracellular ATP concentration (µM) measured by luminometric assay in splenic $CD19^+$ cells. **(I)** Bar histogram shows the adenosine concentration (µM) measured by fluorometric assay in the plasma of the indicated group of mice. **(J)** Histogram showing the percentage of $LAG3^+$ PB/PC among live cells in the spleen of each indicated group of animals. **(K)** Relative *Il10* mRNA expression measured in splenic $CD19^+$ cells from the indicated group of animals. Relative expression was normalized to *B2m*. Bars represent median ± min to max. **(B-K)** Combined data from 2 independent experiments, each performed with 4–5 mice per group, are shown. Bars represent means ± SEM. Symbols represent one individual mouse. * $p<0.05$, ** $p<0.01$, *** $p<0.001$ (**B-E**: Kruskal-Wallis test, **F-K**: Mann-Whitney test).

© 2022 The Authors. *European Journal of Immunology* published by Wiley-VCH GmbH

15214141, 2023, 3, Downloaded from https://onlinelibrary.wiley.com/doi/10.1002/eji.202250154 by Université De Rennes 1 BU Campus Beaulieu - Bât. 40, Wiley Online Library on [04/07/2023]. See the Terms and Conditions (https://onlinelibrary.wiley.com/terms-and-conditions) on Wiley Online Library for rules of use; OA articles are governed by the applicable Creative Commons License

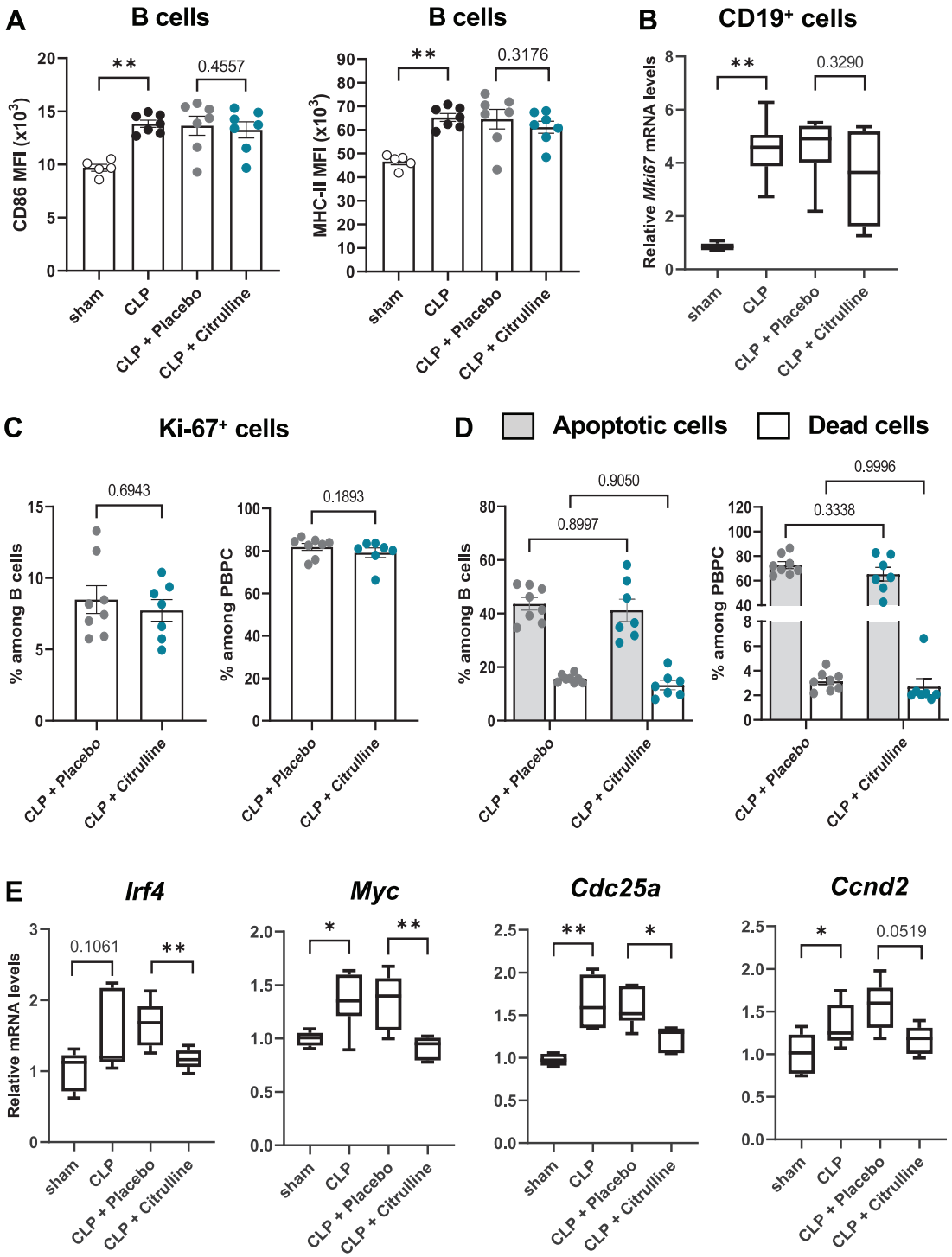

Figure 4. Citrulline diet shapes B cell response away from an EF PC differentiation. (A) Histograms show the MFI of CD86 (left) and MHC-II (right) measured in splenic B cells ($CD19^+$ $B220^+$ $TACI^-$ $CD138^-$) of sham, CLP, CLP + placebo, and CLP + citrulline mice (5-7 mice per group, N = 1). **(B)** Relative *Mki67* mRNA expression measured in splenic $CD19^+$ cells from the indicated group of animals (5-7 mice per group). Relative expression was normalized to *B2m*. Bars represent median ± min to max. **(C)** Histograms show the percentage of Ki-67^+ cells among B cells ($CD19^+$ $B220^+$; on left) and among PB/PC ($TACI^+$ $CD138^+$; on right) on CLP + placebo and CLP + citrulline mice (8 and 7 mice per group, respectively, one experiment representative of 2). **(D)** Histograms represent the percentage of $AnnexinV^+$ $DAPI^-$ apoptotic cells (gray bars) and the percentage of $AnnexinV^+$ $DAPI^+$ dead cells (white bars) among B cells (left) and among PB/PC (right) of each group of animals (8 and 7 mice per group, respectively, one experiment representative of 2, two-way ANOVA with Tukey correction). **(E)** Relative mRNA expression of *Irf4*, *Myc*, *Cdc25a*, and *Ccnd2* measured in splenic $CD19^+$ cells from the indicated group of animals (5-7 mice per group). Relative expression was normalized to *B2m*. Box plot Bars represent median ± min to max. **(A, C, D)** Symbols represent one individual mouse. Data are presented as mean ± SEM. * $p<0.05$, ** $p<0.01$, *** $p<0.001$ (Mann-Whitney test between sham and CLP or CLP + placebo and CLP + citrulline, without joint interpretation, unless specified).

© 2022 The Authors. *European Journal of Immunology* published by Wiley-VCH GmbH

15214141, 2023, 3, Downloaded from https://onlinelibrary.wiley.com/doi/10.1002/eji.202250154 by Université De Rennes 1 BU Campus Beaulieu - Bât. 40, Wiley Online Library on [04/07/2023]. See the Terms and Conditions (https://onlinelibrary.wiley.com/terms-and-conditions) on Wiley Online Library for rules of use; OA articles are governed by the applicable Creative Commons License

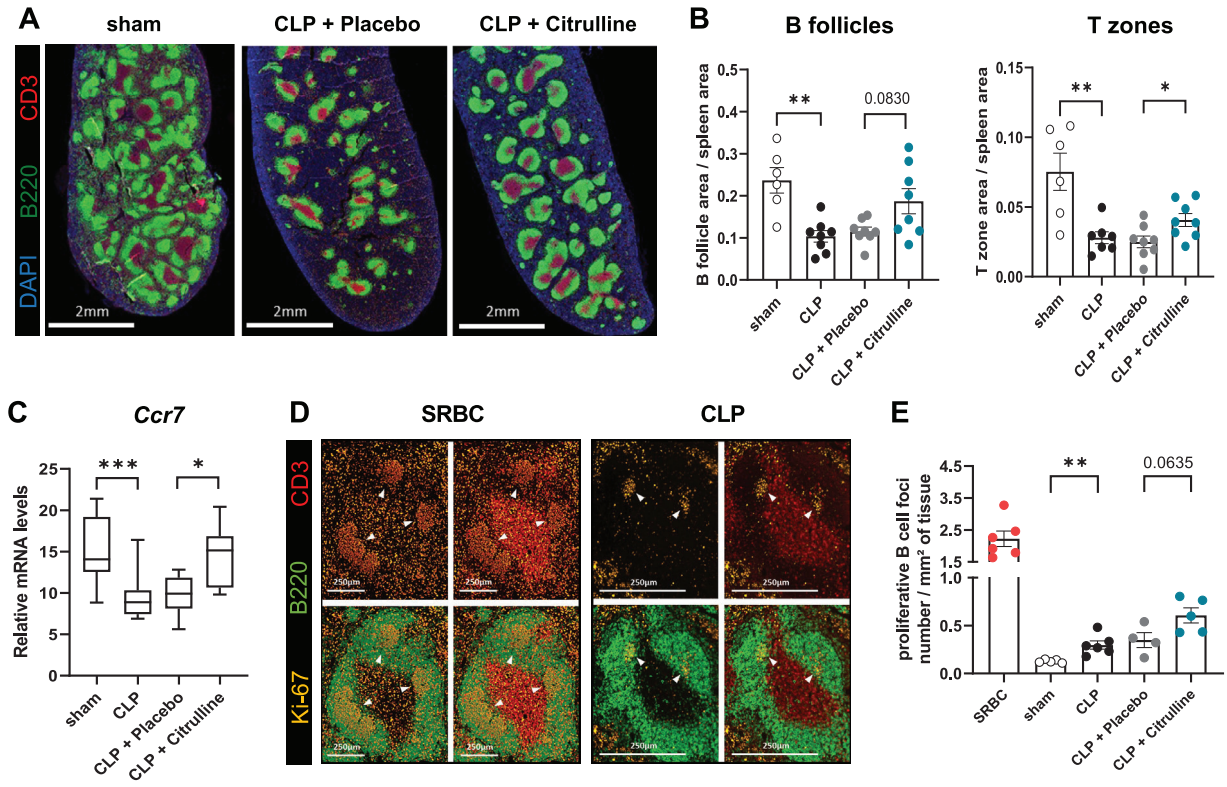

Figure 5. Citrulline diet restores the splenic architecture required for T-dependent B cell responses. (A) Immunofluorescences of representative splenic tissue sections from sham, CLP + placebo, and CLP + citrulline mice (6-9 mice per group combined from 2 independent experiments). Sections of spleens are stained with DAPI (blue) and antibodies targeting B220 (green) and CD3 (red). Scale bars, 2 mm. **(B)** Graphs represent the ratio of the B follicle area or T zone area to the total spleen section area. Combined data from 2 independent experiments, each performed with 3–4 mice per group, are shown. **(C)** Relative *Ccr7* mRNA expression measured in splenic cells from the indicated group of animals (5-7 mice per group). Relative expression was normalized to *B2m*. Box plot represents median ± min to max. **(D)** Representative immunofluorescences of splenic tissue sections from SRBC-immunized and CLP mice (5-6 mice per group). Proliferative B cell foci within B cell follicles are indicated with white arrows. The splenic tissue sections are stained with an anti-B220 (green), an anti-CD3 (red), and an anti-Ki-67 (yellow). Scale bars, 250 µm. **(E)** Graph represents the proliferative B cell foci number per mm^2 of splenic tissue sections in SRBC immunized mice, sham, CLP, and mice in the different diet groups (5-6 mice per group). **(B, E)** Bars represent means ± SEM. Symbols represent one individual mouse. * $p<0.05$, ** $p<0.01$, *** $p<0.001$ (Mann-Whitney test between sham and CLP or CLP + placebo and CLP + citrulline, without joint interpretation).

receptor involved in lymphocyte homing and migration significantly reduced in splenocytes following CLP compared to sham ($p = 0.0008$), was rescued with citrulline diet ($p = 0.0152$; Fig. 5C). At least, compared to sheep red blood cell immunized mice used as a control for GC formation, very few small and early GCs defined here as Ki-67$^+$ B220$^+$ foci within B cell follicles were formed following CLP in agreement with a dominant EF response (Fig. 5D). However, an average 2-fold increase in the number of early GCs was observed in spleen following CLP and citrulline enriched diet compared to CLP and placebo ($p = 0.0635$; Fig. 5E). Altogether our results suggest that citrulline diet shunts the dominant EF B cell response associated with immunosuppression in sepsis and restores the splenic architecture required for T-dependent B cell responses (Fig. 6).

Discussion

B cells, whose functions may be polarized toward pro-inflammatory or regulatory responses, have important emerging roles in the sustained immunosuppression induced in sepsis [4, 16]. In this study, we analyzed the effect of citrulline diet on B cell-mediated immunosuppression in the CLP model of sepsis. We showed that citrulline administration counteracts the dominant EF PC differentiation that correlates with immunosuppressive B cell responses and splenic architecture disorganization induced by sepsis.

First, we confirmed that arginine deficiency was restored with citrulline diet [23]. In agreement with lymphopenia observed in sepsis [3, 29], we observed a significant decrease in B cell frequency in the spleen of CLP compared to sham mice 5 days post-surgery. Citrulline administration, though, failed to reverse B cell depletion of the spleen.

Importantly, we described a dominant EF B cell response in sepsis, detrimental to spleen morphology and GC response. The disruption of normal splenic architecture is a characteristic of EF response following infection that may contribute to GC suppression [30, 31]. Our observation is consistent with the reduced antigen-specific primary antibody response described in CLP [2, 3] and the impaired humoral responses in sepsis survivors [11].

© 2022 The Authors. *European Journal of Immunology* published by Wiley-VCH GmbH

15214141, 2023, 3, Downloaded from https://onlinelibrary.wiley.com/doi/10.1002/eji.202250154 by Université De Rennes 1 BU Campus Beaulieu - Bât. 40, Wiley Online Library on [04/07/2023]. See the Terms and Conditions (https://onlinelibrary.wiley.com/terms-and-conditions) on Wiley Online Library for rules of use; OA articles are governed by the applicable Creative Commons License

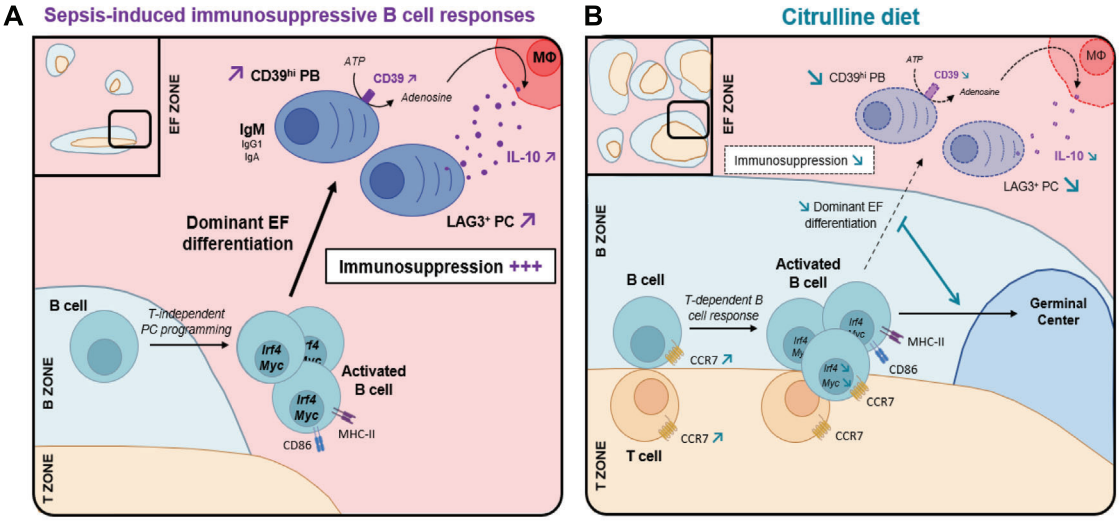

Figure 6. Schematic representation of the effects of the citrulline diet on post-septic immunosuppressive B cell responses. (A) B-cell responses in the spleen of septic mice. Dominant extrafollicular (EF) plasma cell (PC) differentiation correlates with immunosuppressive B cell responses: increased production of $CD39^{hi}$ plasmablasts (PB), $LAG3^{+}$ PC and IL-10 with sepsis (purple arrows), and splenic architecture disorganization: smaller B cell follicles and T cell zones, visualized in the upper left square. **(B)** Citrulline diet shapes B-cell responses away from an EF/immunoregulatory profile. Blue arrows represent the impact of citrulline treatment on cell subsets (either upregulated or downregulated). Decreased $CD39^{hi}$ PB, $LAG3^{+}$ PC compartments and IL-10 production are shown with blue arrows. Splenic architecture required for T-dependent B cell responses is restored (spleen morphology shown in the upper left square). **(A** and **B)** T cells and T cell zone in orange, B cells and B cell follicles in light blue, plasma cells in dark blue, EF zone in pink.

This is also consistent with a previous report showing PC in spleen as soon as day 3 post CLP [29]. This EF response triggered the differentiation of immunosuppressive CD39- and LAG3-expressing PB/PC following CLP that was strongly inhibited in mice receiving citrulline-enriched diet. As a result, a significant decrease in the anti-inflammatory IL-10 cytokine production is expected because IL-10-producing $LAG3^{+}$ PC frequency was lower and because adenosine, which results from CD39-mediated ATP hydrolysis and triggers IL-10-production by macrophages in sepsis [16], did not accumulate. Importantly, IL-10 is a key immunosuppressive cytokine in sepsis [32] and a key mediator of PB/PC suppressive functions following infections [13]. IL-10 was shown to promote Treg expansion and to contribute to the impaired lung host-defence to secondary infection [33]. In line with this, an adenosine increase in septic mice impairs macrophage bacterial killing [16]. We could thus speculate that a citrulline diet may improve macrophage function through the inhibition of the $CD39^{hi}$ PB population, hence contributing to a decrease in the severity of second infections observed in the two-hit model [23]. Whether this initial EF PB response in CLP producing these $CD39^{hi}$ cells continues to expand for weeks to months as it has been shown for *Ehrlichia muris* and *Salmonella enterica* serovar Typhimurium infection [34, 35] remains to be studied. In this regard, it could be responsible for persistent immunosuppression following sepsis.

Terminal B cell differentiation is intermingled with B cell proliferation, critical early B cell fate reprogramming, and metabolic shift towards glycolysis and oxidative phosphorylation to support the increased metabolic demands [25, 36]. Mechanistically, we demonstrated that citrulline administration did not significantly impact the activation or proliferation of splenic B cells triggered by CLP. The viability of splenic B cells and PB/PC was unaffected. In line with this, and in agreement with the absence of B-cell intrinsic defects in CLP mice [11], it was unlikely that citrulline treatment affected PC differentiation by a B cell intrinsic mechanism. In contrast, we found that the IRF4/MYC-mediated B cell fate commitment towards PC differentiation was shunted possibly into a GC response with citrulline diet. MYC is a well-known transcription factor that regulates the B cell proliferative response [37]. MYC target genes such as *Ccnd2* [38] and the crucial cell cycle regulator *Cdc25a* [39] were indeed downregulated with citrulline diet. Both *Irf4* and *Myc* induction levels in B cells depend on the strength and nature of signaling from the microenvironment [40, 41]. We found here that citrulline diet promoted reappearance of B and T follicles, making it possible cell interactions of multiple cell types required for the formation of GCs [42]. Supporting B cell–T cell interactions, we found that *Ccr7* expression, an important organizer of B cell response [43], was rescued with citrulline. Following BCR priming, activated B cells increase their expression of *Ccr7* to relocate at the T-B border, where they received help from T cells required to initiate the GC reaction [44]. Since we have shown previously that citrulline administration restores T cell mitochondrial function and proliferation [23], T cell function retrieval may shape B cell responses toward GC formation at the expense of EF PC differentiation.

Although our study was not designed to study sepsis-related mortality, we did not observe a difference in mortality between the placebo and citrulline diet groups, suggesting no major impact of Ig depletion on sepsis outcome in the initial host response.

© 2022 The Authors. *European Journal of Immunology* published by Wiley-VCH GmbH

15214141, 2023, 3, Downloaded from https://onlinelibrary.wiley.com/doi/10.1002/eji.202250154 by Université De Rennes 1 BU Campus Beaulieu - Bât. 40, Wiley Online Library on [04/07/2023]. See the Terms and Conditions (https://onlinelibrary.wiley.com/terms-and-conditions) on Wiley Online Library for rules of use; OA articles are governed by the applicable Creative Commons License

Along these lines, a large study on 956 patients with severe sepsis and septic shock concluded that high levels of IgA and IgG on the first day of diagnosis were associated with decreased 90-day survival, while no association was found between IgM and survival [45]. Furthermore, the role of intravenous immunoglobulins during sepsis is controversial as inconsistent survival benefits have been observed [46]. Taken altogether, we believe that a decreased Ig concentration with citrulline diet would unlikely contribute to the worst outcome in sepsis. In contrast, impaired B cell response has been associated with late mortality from secondary infections [4, 47]. Thus, our data demonstrating that citrulline diet markedly counteracts sepsis-induced B cell impairment suggest that citrulline diet could potentially participate in the better outcome previously reported [23].

Our observations also suggest that overcoming arginine shortage through citrulline administration might prevent non-specific and auto-reactive anti-DNA antibodies detected previously in the primary response of septic mice [2] and foster an effective antigen-specific response within GCs. These are important processes in the resolution of infection that require future studies. Cytokines are major inputs driving B cell fate destiny toward EF versus GC paths [8]. Further research on this axis is needed to determine the mechanisms driven by citrulline supplementation. Furthermore, we cannot exclude that citrulline complementation impacts B cell subsets at steady state.

Altogether, we have evidence that citrulline enriched diet may act in concert in B and T cell effector and regulatory subsets to restore B and T cell homeostasis and to decrease immune dysfunction after inflammatory activation. The clinical relevance of our findings has to be investigated.

Materials and methods

Ethics approval statement for animal studies

All the experiments were approved by the Institutional Animal Care and Use Committee of Rennes and by the French Ministry of Education and Research in accordance with the European Convention for the Protection of Vertebrate Animals used for Experimental and Other Scientific Purposes (Approval No.9746-2017042717414943).

Animals

C57BL/6J mice (10-week-old females) were purchased from Janvier Labs (Le Genest Saint Isle, France). These mice underwent CLP or sham surgery, as previously reported [23]. Before surgery, mice were anesthetized with isoflurane and received a buprenorphine intra-muscular injection (100μg/kg). An intraperitoneal injection of antibiotic (25mg/kg meropenem) was initiated 6 h after surgery and repeated daily for 5 days. Saline solution for fluid resuscitation and buprenorphine for pain relief was administered, respectively, at the end or 6 hours after surgery. The mice were monitored twice a day to ensure animal welfare. CLP animals received immunonutrition treatment by oral gavage with arginine (150mg/kg), citrulline (150mg/kg) or an isonitrogenous placebo once a day for 4 days. All mice were sacrificed at day 5.

One group of naive mice received an intraperitoneal injection (200 μL) of 2×10^9 SRBC (Sheep Red Blood Cells). These mice were sacrificed on day 5 post-injection. Spleens were recovered for immunofluorescence analysis.

Sample preparation

Five days after surgery, mice were anesthetized with isoflurane, whole blood was obtained by direct cardiac puncture, and recovered in sterile heparinized tube. The mice were then euthanized by cervical dislocation and opened to recover the spleen.

Blood samples were centrifuged at 480 × *g*, 5 min before plasma was centrifuged at 3200 × *g*, 5 min, 20°C to recover the plasma samples. These samples were stored at −80°C, pending their use.

Spleens were crushed in PBS-2% FBS (Gibco, 10270-106) on a 40 μm filter placed over a 50 mL tube. Cells were pelleted and resuspended in 3 mL Easylyse (DAKO, S2364) for 10 min at room temperature to lyse the red blood cells. Cells were pelleted, then resuspended in PBS-2% FBS, and filtered before counting.

$CD19^+$ cells isolation

Splenic $CD19^+$ cells were isolated using CD19 Microbeads, mouse (Miltenyi, 130-121-301). Purity was checked by flow cytometry using an anti-CD19-APC-Vio770 (Miltenyi) and DAPI labeling (Sigma-Aldrich). $CD19^+$ cells were counted and used for intracellular ATP measurement and gene expression quantification (qPCR).

Flow cytometry

One million splenocytes were labeled for 30 minutes at 4°C with antibodies listed in Table S1. Before analysis, DAPI (Sigma-Aldrich) was added to exclude dead cells. For intracellular staining, cells were first labelled with LIVE/DEAD™ Fixable Violet Dead Cell Stain Kit (ThermoFisher Scientific, L34955) according to the manufacturer's recommendations. Then, extracellular staining was performed with the required antibodies. Finally, a transcription factor staining buffer set (Miltenyi, 130-122-981) was used to fix and permeabilize cells before intracellular staining with anti-Ki-67 antibody. For apoptosis analysis, the cells were stained with FITC-AnnexinV (Tau Technologies, A700) and DAPI (Sigma Aldrich). $AnnexinV^+$ $DAPI^-$ cells were considered apoptotic and $AnnexinV^+$ $DAPI^+$ cells were considered dead. All tubes were analyzed on the CytoFlex (Beckman Coulter). Gating

© 2022 The Authors. European Journal of Immunology published by Wiley-VCH GmbH

15214141, 2023, 3, Downloaded from https://onlinelibrary.wiley.com/doi/10.1002/eji.202250154 by Université De Rennes 1 BU Campus Beaulieu - Bât. 40, Wiley Online Library on [04/07/2023]. See the Terms and Conditions (https://onlinelibrary.wiley.com/terms-and-conditions) on Wiley Online Library for rules of use; OA articles are governed by the applicable Creative Commons License

strategies are displayed in Fig. S1. Flow cytometry files were analyzed using FlowJo software v10.6.2.

Cell sorting

Five million splenocytes were labeled with CD138-PE-Vio770, TACI-FITC, B220-PerCP-Vio700, CD19-APC-Vio770, Lag3-PE (Table S1), 30 min at 4°C. Five thousand $CD138^+$ $TACI^+$ living cells (PB/PC), $CD138^+$ $TACI^+$ $LAG3^-$ living cells (PB/PC $Lag3^-$) or $CD19^+$ $B220^+$ $CD138^-$ $TACI^-$ living cells (B cells) were sorted directly in flat bottom 96-well plate and cultured during 24 h at 37°C, 5% of CO_2 in the presence of 5ng/mL LPS (eBioscience, 004976–93) and 10μg/mL F(ab')2-Goat-anti-Mouse IgM (eBioscience, 16-5092-85) in 100 μL standard complete media (RPMI 1640 Medium GlutaMAX supplement (Gibco, 61870010), 10% of decomplemented FBS, 1× penicillin/streptomycin (Gibco, 15140130), 1 mM sodium pyruvate (Gibco, 11360039), 1× non-essential amino acid (Gibco, 11140035), 10 mM HEPES pH 7.4 (Gibco, 15630-049), 50 μM 2-mercaptoethanol (Gibco, 21985023). At the end of the culture, cells were pelleted, and culture supernatants were recovered and stored at −80°C.

Dosage

IL-10 dosage

IL-10 was measured in cell culture supernatants using a LEGEND MAX Mouse IL-10 ELISA Kit (BioLegend, 431417). According to the manufacturing recommendations, 50μL of pure supernatants were used, and the plate was read at 450 nm on the microplate reader 680 (Bio-Rad).

ATP dosage

ATP was measured on isolated splenic $CD19^+$ cells using a Luminescent ATP Detection Assay Kit (Abcam, ab113849). Briefly, $CD19^+$ cells were resuspended in complete RPMI media without phenol red (Gibco, 11835063) at 5×10^5 cells/mL. A total of 5×10^4 $CD19^+$ cells were dispensed in a white flat bottom plate. The ATP dosage was performed according to the manufacturer's recommendations. The luminescent signal was measured on Varioskan (ThermoFisher Scientific). An ATP standard curve was used to determine the ATP concentration.

Adenosine dosage

Adenosine was dosed on plasma samples using an Adenosine Quantification Assay Kit (Sigma, MAK433-1KT). According to the manufacturing recommendations, we used 20 μL of frozen plasma samples to measure adenosine concentration. The plate was read on Varioskan (ThermoFisher Scientific). The fluorescent product was excited at 535 nm and detected at 587 nm.

Immunoglobulin dosage

Immunoglobulins were dosed on plasma samples using Luminex technology with Antibody Isotyping 7-Plex Mouse ProcartaPlex™ Panel (ThermoFisher Scientific, EPX070-20815-901). Plasma samples were diluted to 1/10,000 before use. The plate was read on Bio-Plex 200 (Bio-Rad).

Arginine dosage

Arginine quantity was determined by liquid chromatography coupled with tandem mass spectrometry (LC–MS/MS).

Immunofluorescence

Five days after CLP or SRBC immunizations, spleens were recovered, fixed in 4% PFA for 48 h, and paraffin embedded. Splenic tissue sections (4 μm) were labeled with diluted anti-B220, anti-CD3, anti-Ki-67, anti-CD138, anti-IgM, and/or DAPI (Table S2) with a multiplex immunofluorescence labeling technique using the DISCOVERY XT Ventana (Roche Diagnostics, Meylan, France). The marked slides were scanned using a digital slide scanner Nanozoomer 2.0 RS (Hamamatsu, magnification: 20X, resolution: 0.46 μm/pixel) and visualized on NDPView2 software (Hamamatsu). Quantification analyses were performed using ImageJ software 1.53a.

Real-time qPCR

RNAs were extracted from $CD19^+$ splenic cells or the total spleen using NucleoSpin RNA Plus XS (Macherey-Nagel, 740990.50). cDNA synthesis was performed with SuperScript II reverse transcriptase and random primers (Thermo Fisher Scientific, 18064014 and 48190011). For qRT-PCR, we used 1× of *B2m*, *Il10*, *Mki67, Irf4, Myc, Cdc25a*, *Ccnd2*, and *Ccr7* TaqMan® Gene Expression Assay (Table S3) and Taqman Universal Master Mix (Thermo Fisher Scientific, 4304437). Gene expression was measured using StepOnePlus (Bio-Rad) based on the ΔCt calculation method. *B2m* was used as an endogenous control. For each gene, relative expression to *B2m* was determined, and the average expression of the sham group fixed to 1.

Statistics

All statistical tests were performed on GraphPad Prism 9.3.1. Unpaired multi-group comparisons with one variable were performed using the Kruskal–Wallis nonparametric test. Multi-group comparisons with two variables were performed with two-way ANOVA with Tukey correction. Paired comparison with one variable was performed using the Wilcoxon non-parametric test. Differences between sham and CLP or CLP + placebo and CLP

© 2022 The Authors. *European Journal of Immunology* published by Wiley-VCH GmbH

15214141, 2023, 3, Downloaded from https://onlinelibrary.wiley.com/doi/10.1002/eji.202250154 by Université De Rennes 1 BU Campus Beaulieu - Bât. 40, Wiley Online Library on [04/07/2023]. See the Terms and Conditions (https://onlinelibrary.wiley.com/terms-and-conditions) on Wiley Online Library for rules of use; OA articles are governed by the applicable Creative Commons License

+ citrulline were evaluated by Mann–Whitney (nonparametric unpaired T-test). We did not perform a joint interpretation in this case. For correlation analysis, the Pearson test was used. The *p*-values < 0.05 were considered statistically significant: **p*-value < 0.05; ***p*-value < 0.01; ****p*-value < 0.001; *****p*-value < 0.0001. Ns, non-significant (*p*-value > 0.05).

Acknowledgments: This work was in part funded by an ANR JCJC grant (ANR-18-CE15-0002-01) and a grant from LabEx IGO program (ANR-11-LABX-0016-01) funded by the "Investissements d'Avenir" French Government program, managed by the French National Research Agency (ANR) to CD. We thank the animal housing facility ARCHE, the H2P2 platform for help with tissue staining, and the Flow cytometry and cell sorting platform from BIOSIT (UAR 3480 CNRS - US018 INSERM).

Conflict of interest disclosure: The authors declare no commercial or financial conflict of interest.

Author contributions: Conception and design, experiments, data analysis, and interpretation were provided by JG, FR, MG, ML, YD, CM, GG, JMT, and CD. Drafting and revision of the manuscript were carried out by JG, FR, MG, ML, PA, KT, JMT, and CD, with all authors providing critical feedback and edits to subsequent revisions.

Data availability statement: The data that supports the findings are included in the article and supplementary information of this article.

Peer review: The peer review history for this article is available at https://publons.com/publon/10.1002/eji.202250154

References

1 **Hotchkiss, R. S., Monneret, G. and Payen, D.**, Sepsis-induced immunosuppression: from cellular dysfunctions to immunotherapy. *Nat. Rev. Immunol.* 2013. **13**: 862–874.

2 **Mohr, A., Polz, J., Martin, E. M., Grießl, S., Kammler, A., Pötschke, C., Lechner, A. et al.**, Sepsis leads to a reduced antigen-specific primary antibody response. *European Journal of Immunology*. 2012, **42**: 341–352.

3 **Sjaastad, F. V., Condotta, S. A., Kotov, J. A., Pape, K. A., Dail, C., Danahy, D. B., Kucaba, T. A. et al.**, Polymicrobial Sepsis Chronic Immunoparalysis Is Defined by Diminished Ag-Specific T Cell-Dependent B Cell Responses. *Front. Immunol.* 2018. **9**. Available at: https://www.frontiersin.org/article/10.3389/fimmu.2018.02532 [Accessed April 19, 2022].

4 **Gustave, C.-A., Gossez, M., Demaret, J., Rimmelé, T., Lepape, A., Malcus, C., Poitevin-Later, F. et al.**, Septic Shock Shapes B Cell Response toward an Exhausted-like/Immunoregulatory Profile in Patients. *J. Immunol.* 2018. **200**: 2418–2425.

5 **Hotchkiss, R. S., Tinsley, K. W., Swanson, P. E., Schmieg, R. E., Hui, J. J., Chang, K. C., Osborne, D. F. et al.**, Sepsis-Induced Apoptosis Causes Progressive Profound Depletion of B and CD4+ T Lymphocytes in Humans. *J. Immunol.* 2001. **166**: 6952–6963.

6 **Venet, F., Davin, F., Guignant, C., Larue, A., Cazalis, M.-A., Darbon, R., Allombert, C. et al.**, Early assessment of leukocyte alterations at diagnosis of septic shock. *Shock* 2010. **34**: 358–363.

7 **Hotchkiss, R. S., Osmon, S. B., Chang, K. C., Wagner, T. H., Coopersmith, C. M. and Karl, I. E.**, Accelerated lymphocyte death in sepsis occurs by both the death receptor and mitochondrial pathways. *J. Immunol.* 2005. **174**: 5110–5118.

8 **Elsner, R. A. and Shlomchik, M. J.**, Germinal Center and Extrafollicular B Cell Responses in Vaccination, Immunity, and Autoimmunity. *Immunity* 2020. **53**: 1136–1150.

9 **Wiggins, K. J. and Scharer, C. D.**, Roadmap to a plasma cell: epigenetic and transcriptional cues that guide B cell differentiation. *Immunol. Rev.* 2021. **300**: 54–64.

10 **Weisel, F. J., Mullett, S. J., Elsner, R. A., Menk, A. V., Trivedi, N., Luo, W., Wikenheiser, D. et al.**, Germinal center B cells selectively oxidize fatty acids for energy while conducting minimal glycolysis. *Nat. Immunol.* 2020. **21**: 331–342.

11 **Rana, M., Bella, A. L., Lederman, R., Volpe, B. T., Sherry, B. and Diamond, B.**, Follicular dendritic cell dysfunction contributes to impaired antigen-specific humoral responses in sepsis-surviving mice. *J. Clin. Invest.* 2021; **131**: e146776. Available at: https://www.jci.org/articles/view/146776 [Accessed July 19, 2022].

12 **Matsushita, T.**, Regulatory and effector B cells: Friends or foes? *J. Dermatol. Sci.* 2019. **93**: 2–7.

13 **Neves, P., Lampropoulou, V., Calderon-Gomez, E., Roch, T., Stervbo, U., Shen, P., Kühl, A. A. et al.**, Signaling via the MyD88 Adaptor Protein in B Cells Suppresses Protective Immunity during Salmonella typhimurium Infection. *Immunity* 2010. **33**: 777–790.

14 **Fillatreau, S.**, Regulatory functions of B cells and regulatory plasma cells. *Biomed J.* 2019. **42**: 233–242.

15 **Delaloy, C., Schuh, W., Jäck, H.-M., Bonaud, A. and Espéli, M.**, Single-cell resolution of plasma cell fate programming in health and disease. *Eur. J. Immunol.* 2022. **52**: 10–23.

16 **Nascimento, D. C., Viacava, P. R., Ferreira, R. G., Damaceno, M. A., Piñeros, A. R., Melo, P. H., Donate, P. B. et al.**, Sepsis expands a CD39+ plasmablast population that promotes immunosuppression via adenosine-mediated inhibition of macrophage antimicrobial activity. *Immunity* 2021. **54**: 2024–2041.e8.

17 **Harada, Y., Kawano, M. M., Huang, N., Mahmoud, M. S., Lisukov, I. A., Mihara, K., Tsujimoto, T. et al.**, Identification of early plasma cells in peripheral blood and their clinical significance. *Br. J. Haematol.* 1996. **92**: 184–191.

18 **Lino, A. C., Dang, V. D., Lampropoulou, V., Welle, A., Joedicke, J., Pohar, J., Simon, Q. et al.**, LAG-3 Inhibitory Receptor Expression Identifies Immunosuppressive Natural Regulatory Plasma Cells. *Immunity* 2018. **49**: 120–133.e9.

19 **Collins, N., Belkaid, Y.**, Control of immunity via nutritional interventions. *Immunity* 2022. **55**: 210–223.

20 **Gey, A., Tadie, J.-M., Caumont-Prim, A., Hauw-Berlemont, C., Cynober, L., Fagon, J.-Y., Terme, M. et al.**, Granulocytic myeloid-derived suppressor cells inversely correlate with plasma arginine and overall survival in critically ill patients. *Clin. Exp. Immunol.* 2015. **180**: 280–288.

21 **Wijnands, K. A. P., Castermans, T. M. R., Hommen, M. P. J., Meesters, D. M. and Poeze, M.**, Arginine and Citrulline and the Immune Response in Sepsis. *Nutrients* 2015. **7**: 1426–1463.

© 2022 The Authors. *European Journal of Immunology* published by Wiley-VCH GmbH

15214141, 2023, 3, Downloaded from https://onlinelibrary.wiley.com/doi/10.1002/eji.202250154 by Université De Rennes 1 BU Campus Beaulieu - Bât. 40, Wiley Online Library on [04/07/2023]. See the Terms and Conditions (https://onlinelibrary.wiley.com/terms-and-conditions) on Wiley Online Library for rules of use; OA articles are governed by the applicable Creative Commons License

22 **Westhaver, L. P., Nersesian, S., Nelson, A., MacLean, L. K., Carter, E. B., Rowter, D., Wang, J. et al.**, Mitochondrial damage-associated molecular patterns trigger arginase-dependent lymphocyte immunoregulation. *Cell Rep.* 2022. **39**: 110847.

23 **Reizine, F., Grégoire, M., Lesouhaitier, M., Coirier, V., Gauthier, J., Delaloy, C., Dessauge, E. et al.**, Beneficial effects of citrulline enteral administration on sepsis-induced T cell mitochondrial dysfunction. *Proc. Natt. Acad. Sci.* 2022. **119**: e2115139119.

24 **Pracht, K., Meinzinger, J., Daum, P., Schulz, S. R., Reimer, D., Hauke, M., Roth, E. et al.**, A new staining protocol for detection of murine antibody-secreting plasma cell subsets by flow cytometry. *Eur. J. Immunol.* 2017. **47**: 1389–1392.

25 **Scharer, C. D., Patterson, D. G., Mi, T., Price, M. J., Hicks, S. L. and Boss, J. M.**, Antibody-secreting cell destiny emerges during the initial stages of B-cell activation. *Nat. Commun.* 2020. **11**: 3989.

26 **Ochiai, K., Maienschein-Cline, M., Simonetti, G., Chen, J., Rosenthal, R., Brink, R., Chong, A. S. et al.**, Transcriptional Regulation of Germinal Center B and Plasma Cell Fates by Dynamical Control of IRF4. *Immunity* 2013. **38**: 918–929.

27 **Patterson, D. G., Kania, A. K., Price, M. J., Rose, J. R., Scharer, C. D. and Boss, J. M.**, An IRF4–MYC–mTORC1 Integrated Pathway Controls Cell Growth and the Proliferative Capacity of Activated B Cells during B Cell Differentiation In Vivo. *J. Immunol.* 2021. **207**: 1798–1811. Available at: https://www.jimmunol.org/content/early/2021/09/01/jimmunol.2100440 [Accessed April 19, 2022].

28 **Xu, H., Chaudhri, V. K., Wu, Z., Biliouris, K., Dienger-Stambaugh, K., Rochman, Y. and Singh, H.** Regulation of bifurcating B cell trajectories by mutual antagonism between transcription factors IRF4 and IRF8. *Nat. Immunol.* 2015. **16**: 1274–1281

29 **Taylor, M. D., Brewer, M. R., Nedeljkovic-Kurepa, A., Yang, Y., Reddy, K. S., Abraham, M. N., Barnes, B. J. et al.**, CD4 T Follicular Helper Cells Prevent Depletion of Follicular B Cells in Response to Cecal Ligation and Puncture. *Front. Immunol.* 2020. **11**: 1946. Available at: https://www.frontiersin.org/article/10.3389/fimmu.2020.01946 [Accessed April 19, 2022].

30 **Di Niro, R., Lee, S.-J., Vander Heiden, J. A., Elsner, R. A., Trivedi, N., Bannock, J. M., Gupta, N. T. et al.**, Salmonella Infection Drives Promiscuous B Cell Activation Followed by Extrafollicular Affinity Maturation. *Immunity* 2015. **43**: 120–131.

31 **Popescu, M., Cabrera-Martinez, B. and Winslow, G. M.**, TNFα contributes to lymphoid tissue disorganization and GC B cell suppression during intracellular bacterial infection. *J. Immunol.* 2019. **203**: 2415–2424.

32 **Steinhauser, M. L., Hogaboam, C. M., Kunkel, S. L., Lukacs, N. W., Strieter, R. M. and Standiford, T. J.**, IL-10 is a major mediator of sepsis-induced impairment in lung antibacterial host defense. *J. Immunol.* 1999. **162**: 392–399.

33 **Nascimento, D. C., Melo, P. H., Piñeros, A. R., Ferreira, R. G., Colón, D. F., Donate, P. B., Castanheira, F. V. et al.**, IL-33 contributes to sepsis-induced long-term immunosuppression by expanding the regulatory T cell population. *Nat. Commun.* 2017. **8**: 14919

34 **Racine, R., Jones, D. D., Chatterjee, M., McLaughlin, M., MacNamara, K. C. and Winslow, G. M.**, Impaired Germinal Center Responses and Suppression of Local IgG Production during Intracellular Bacterial Infection. *J. Immunol.* 2010. **184**: 5085–5093.

35 **Cunningham, A. F., Gaspal, F., Serre, K., Mohr, E., Henderson, I. R., Scott-Tucker, A., Kenny, S. M. et al.**, Salmonella Induces a Switched Antibody Response without Germinal Centers That Impedes the Extracellular Spread of Infection. *J. Immunol.* 2007. **178**: 6200–6207.

36 **Price, M. J., Patterson, D. G., Scharer, C. D. and Boss, J. M.**, Progressive Upregulation of Oxidative Metabolism Facilitates Plasmablast Differentiation to a T-Independent Antigen. *Cell Rep.* 2018. **23**: 3152–3159.

37 **Heinzel, S., Binh Giang, T., Kan, A., Marchingo, J. M., Lye, B. K., Corcoran, L. M. and Hodgkin, P. D.**, A Myc-dependent division timer complements a cell-death timer to regulate T cell and B cell responses. *Nat. Immunol.* 2017. **18**: 96–103.

38 **Bouchard, C., Thieke, K., Maier, A., Saffrich, R., Hanley-Hyde, J., Ansorge, W., Reed, S. et al.**, Direct induction of cyclin D2 by Myc contributes to cell cycle progression and sequestration of p27. *EMBO J.* 1999. **18**: 5321–5333.

39 **Galaktionov, K., Chen, X., Beach, D.**, Cdc25 cell-cycle phosphatase as a target of c-myc. *Nature* 1996. **382**: 511–517.

40 **Sciammas, R., Li, Y., Warmflash, A., Song, Y., Dinner, A. R. and Singh, H.**, An incoherent regulatory network architecture that orchestrates B cell diversification in response to antigen signaling. *Mol. Syst. Biol.* 2011. **7**: 495.

41 **Hawkins, E. D., Oliaro, J., Kallies, A., Belz, G. T., Filby, A., Hogan, T., Haynes, N. et al.**, Regulation of asymmetric cell division and polarity by Scribble is not required for humoral immunity. *Nat. Commun.* 2013. **4**: 1801.

42 **Lu, E. and Cyster, J. G.**, G-protein coupled receptors and ligands that organize humoral immune responses. *Immunol. Rev.* 2019. **289**: 158–172.

43 **Pereira, J. P., Kelly, L. M. and Cyster, J. G.**, Finding the right niche: B-cell migration in the early phases of T-dependent antibody responses. *Int. Immunol.* 2010. **22**: 413–419.

44 **Förster, R., Schubel, A., Breitfeld, D., Kremmer, E., Renner-Müller, I., Wolf, E. and Lipp, M.**, CCR7 coordinates the primary immune response by establishing functional microenvironments in secondary lymphoid organs. *Cell*. 1999. **99**: 23–33.

45 **Alagna, L., Meessen, J., Bellani, G., Albiero, D., Caironi, P., Principale, I., Vivona, L. et al.**, Higher levels of IgA and IgG at sepsis onset are associated with higher mortality: results from the Albumin Italian Outcome Sepsis (ALBIOS) trial. *Ann Intensive Care.* 2021. **11**: 161.

46 **Laupland, K. B., Kirkpatrick, A. W. and Delaney, A.**, Polyclonal intravenous immunoglobulin for the treatment of severe sepsis and septic shock in critically ill adults: a systematic review and meta-analysis. *Crit. Care Med.* 2007. **35**: 2686–2692.

47 **Wang, T., Derhovanessian, A., De Cruz, S., Belperio, J. A., Deng, J. C. and Hoo, G. S.**, Subsequent infections in survivors of sepsis: epidemiology and outcomes. *J. Intensive Care Med.* 2014. **29**: 87–95.

Abbreviations: **CLP**: cecal ligation and puncture · **EF**: extrafollicular · **GC**: germinal center · **PB**: plasmablast · **PC**: plasma cell

Full correspondence: Pr Jean-Marc Tadié, UMR INS1236, Faculté Université de Rennes, 2 Avenue du Pr Léon Bernard 35043 Rennes, France; Dr. Céline Delaloy, UMR INSERM U1236, Faculté de Medecine, Université de Rennes, 2 Av du Pr Leon Bernard, 35043 Rennes, France.
e-mail: jeanmarc.tadie@chu-rennes.fr;
celine.delaloy@univ-rennes1.fr

Received: 26/8/2022
Revised: 22/11/2022
Accepted: 21/12/2022
Accepted article online: 23/12/2022

© 2022 The Authors. *European Journal of Immunology* published by Wiley-VCH GmbH

15214141, 2023, 3, Downloaded from https://onlinelibrary.wiley.com/doi/10.1002/eji.202250154 by Université De Rennes 1 BU Campus Beaulieu - Bât. 40, Wiley Online Library on [04/07/2023]. See the Terms and Conditions (https://onlinelibrary.wiley.com/terms-and-conditions) on Wiley Online Library for rules of use; OA articles are governed by the applicable Creative Commons License